

## Evaluation of the structural and physical properties of $Cd_xZn_{1-x}S$ nanocomposites depending technological condition

L. Gahramanli <sup>a,b,c,\*</sup>, M. Muradov <sup>a</sup>, G. Eyvazova <sup>a</sup>, A. Karimova <sup>a</sup>, M. Jafarov <sup>b</sup>

<sup>a</sup> Nano Research Laboratory, Baku State University, Academic Zahid Khalilov Street 23, Baku, Azerbaijan

<sup>b</sup> Chemical Physics of Nanomaterials, Physics Department, Baku State University, Academic Zahid Khalilov Street 23, Baku, Azerbaijan

<sup>c</sup> NEXT Laboratory, INFN, LNF, Via E. Fermi 54, Frascati, Roma, Italy

The study presents nanocomposite materials based on  $Cd_xZn_{1-x}S$ , synthesized as thin films and nanoparticles through two distinct techniques—sonochemical and SILAR synthesis techniques. The characteristics of these materials were investigated using X-ray diffraction (XRD), Ultraviolet spectroscopy (UV-Vis), Fourier-transform infrared (FTIR) spectroscopy, and Scanning Electron Microscopy (SEM). In the sonochemical approach, samples were prepared with three different stabilizers for comparative analysis to determine influence of type of the stabilizers. Meanwhile, the SILAR approach created thin layers with different components (distinctive  $x$  value- $Cd_xZn_{1-x}S$ ) at various grown temperatures utilizing polyvinyl alcohol (PVA) as a substrate. At the same time, nanocomposite materials compared of same  $x$  value for  $Cd_xZn_{1-x}S$  composite materials by sonochemical and SILAR synthesis technique depending on technological condition.

(Received July 22, 2024; Accepted February 3, 2025)

*Keywords:*  $Cd_xZn_{1-x}S$  nanocomposites, Bands, Crystal structure, Band gap value

### 1. Introduction

II-VI groups' composite elements offer broad potential applications in optics and optoelectronics. Within this group of materials, CdS and ZnS stand out, with band gap value ( $E_g$ ) of 2.42 eV and 3.8 eV, respectively [1]. Introducing dopants or ion-exchanging these compounds in various quantities produces a ternary solid solution, indicated as  $Cd_xZn_{1-x}S$ . Metal nanoparticles have a fundamentally unstable structure under normal conditions because of their high surface energy when dispersed. Stabilizers are used to prevent agglomeration in colloidal systems. The process involves exact interactions between the nanoparticle and the stabilizer. In this case, stabilizers successfully bound the nanoparticle surfaces, preventing coalescence. Many factors, such as concentration, temperature, pH value, reaction medium, and technological circumstances, all substantially impact the physical characteristics and structure of the nanoparticles formed.

PVA, a water-dissolvable, is utilizing as a transparent and aromatic material in the formulation of adhesives, thickening solutions, and stabilizers [2]. PVA has recently been discovered to be useful as a substrate in nanoparticle synthesis, where it plays a stabilizing role by preventing agglomerations. Meanwhile, as a stabilizer, 3-Mercaptopropionic acid (3-MPA) is a transparent, oily chemical molecule that contains both carboxyl and thiol groups. Styrene, generated from benzene, is a clear oily liquid with a high vapor pressure [3].

$Fe_2O_3$  and ternary CdZnS nanoparticles have been used in the literature to modify PVA [4].

The primary goal is to compare the material characteristics of  $Cd_xZn_{1-x}S$  nanoparticles synthesized using sonochemical, and SILAR techniques and various stabilizers that consist of PVA, 3-MPA, and styrene. Research was to assess the impact of technological conditions on the characteristics of the synthesized binary and ternary  $Cd_xZn_{1-x}S$  nanomaterials. The primary objective of this research is to investigate how the characteristics of  $Cd_xZn_{1-x}S$  based nanocomposite materials are altered based on the technological conditions employed in SILAR and sonochemical synthesis techniques. The resulting compounds exhibit advantageous structure and physical properties, and

\* Corresponding author: gahraman.lala@gmail.com

<https://doi.org/10.15251/CL.2025.222.109>

their practical significance lies in the ability to manipulate these properties using different stabilizers and by changing reaction parameters.

The present study was used based on two different synthesis techniques which related to different physical processes. One of them is based on a physical phenomenon that requires high temperature and pressure as a result of the impact on a liquid through ultrasonic waves and occurs due to the cavitation effect, which facilitates the occurrence of chemical bonds. The other process occurs with the formation of layered structures based on the absorption phenomenon. In this regard, the structure of the obtained nanomaterials during their formation, as well as the change of their physical properties depending on the formation mechanism, are also interesting issues. In the literature, there are separate studies of CdZnS nanomaterials using both the sonochemical and SILAR techniques. However, there are no studies on obtaining these structures by two different techniques and comparing their physical properties. From this point of view, the presented work is considered to be one of the interests of conducting a comparative analysis.

## 2. Experimental part

### 2.1. Materials and analysis techniques

The following sections provide comprehensive data on the sonochemical technique for the manufacturing of nanoparticles and the SILAR technique for thin film production:

#### 2.1.1. *Cd<sub>x</sub>Zn<sub>1-x</sub>S-based nanocomposite materials (different x value) production using the sonochemical technique*

For synthesizing nanoparticles, Cd(CH<sub>3</sub>COO)<sub>2</sub>·2H<sub>2</sub>O and Zn(CH<sub>3</sub>COO)<sub>2</sub>·2H<sub>2</sub>O served as the source of cations while Na<sub>2</sub>S·9H<sub>2</sub>O were utilizing as the source of anionic reagent. Cd<sub>x</sub>Zn<sub>1-x</sub>S nanoparticles (x=0.2, 0.4, and 1) were produced using PVA as a stabilizer. For Cd<sub>0.2</sub>Zn<sub>0.8</sub>S nanoparticles (x=0.2), 25 mL, 0.1 M Cd(CH<sub>3</sub>COO)<sub>2</sub>·2H<sub>2</sub>O, 25 mL, 0.4 M Zn(CH<sub>3</sub>COO)<sub>2</sub>·2H<sub>2</sub>O, and 50 mL 0.1 M Na<sub>2</sub>S·9H<sub>2</sub>O solutions prepared. To synthesizing of Cd<sub>0.4</sub>Zn<sub>0.6</sub>S (x=0.4), 25 mL 0.2 M Cd(CH<sub>3</sub>COO)<sub>2</sub>·2H<sub>2</sub>O, 25 mL 0.3 M Zn(CH<sub>3</sub>COO)<sub>2</sub>·2H<sub>2</sub>O, and 50 mL 0.1 M Na<sub>2</sub>S·9H<sub>2</sub>O solutions used [1]. When x=1, CdS nanoparticles formed where prepared 50 mL 0.1 M Cd(CH<sub>3</sub>COO)<sub>2</sub>·2H<sub>2</sub>O and 50 mL 0.1 M Na<sub>2</sub>S·9H<sub>2</sub>O solutions prepared. Distilled water used as the solvent in each reaction. To eliminate oxygen from the reaction medium, continuous nitrogen gas was applied, and the reaction proceeded a duration of two hours. The resulting solutions underwent 3 washes with purified water through centrifugation at 3200 rpm, followed by additional washing with ethanol, and finally, drying at ambient temperature.

#### 2.1.2. *Cd<sub>0.4</sub>Zn<sub>0.6</sub>S-based nanocomposite materials as nanoparticles incorporating three stabilizers production using the sonochemical technique*

Cd<sub>0.4</sub>Zn<sub>0.6</sub>S nanoparticles were produced using the sonochemical technique, employing three distinct stabilizers: PVA, 3-MPA, and styrene. The goal is to determine how these stabilizers affect the characteristics of nanoparticles. Fabrication of Cd<sub>0.4</sub>Zn<sub>0.6</sub>S nanocomposite materials with different stabilizers involves utilizing the specified initial reagents in the indicated proportions. The stabilizer concentration was selected as 7%.

#### 2.1.3. *Cd<sub>x</sub>Zn<sub>1-x</sub>S/PVA based nanocomposite materials as thin film by SILAR technique*

The Cd<sub>x</sub>Zn<sub>1-x</sub>S ternary thin film (x=0.1, 0.2, and 1) with diverse compositions was deposited onto a PVA polymer matrix substrate using the SILAR technique. The goal was to investigate how Cd<sub>x</sub>Zn<sub>1-x</sub>S based nanocomposite materials form by changing x values in the sorption centers of the PVA polymer matrix and to analyze how this process changes at various growth temperatures (T=25°C, 45°C and 65°C).

Initially, thin films produced at room temperature at x=0.1, 0.2, and 1. For x=0.2, Cd(CH<sub>3</sub>COO)<sub>2</sub>·2H<sub>2</sub>O and Zn(CH<sub>3</sub>COO)<sub>2</sub>·2H<sub>2</sub>O were utilized as source of cations, with 25 mL 0.01 M Cd<sup>2+</sup> and 25 mL 0.01 M Zn<sup>2+</sup> serving as cationic sources, respectively. Na<sub>2</sub>S·9H<sub>2</sub>O utilized as source of anion, and glycol alcohol (EG) solution utilized as a washing agent and solvent. In case of x=0.1, 25 mL 0.01 M Cd<sup>2+</sup> source, 25 mL 0.09 M Zn<sup>2+</sup> source, and 50 mL 0.1 M S<sup>2-</sup> source were

utilized. For  $x=1$ , a 50 mL 0.1 M  $\text{Cd}^{2+}$  source and 50 mL 0.1 M  $\text{S}^{2-}$  anion source was used for all samples.

## 2.2. Analysis techniques

The Rigaku Milinflex 250 instrument was used to conduct structural investigation on the materials using the XRD technique.

Optical characteristics were investigated using the UV-VIS Specord 250 spectrophotometer. The Agilent Cary 630 FTIR Spectrometer was used to identify the chemical bonds, while the Vegan Tesca SEM was used to determine morphology.

## 3. Results and discussion

### 3.1. Structural analysis

XRD was employed to conduct structural analysis on all samples, investigating the samples' formation mechanism. Figure 1 displays the diffraction pattern of  $\text{Cd}_x\text{Zn}_{1-x}\text{S}$  ( $x=0.2$  and  $0.4$ ) samples synthesized by the sonochemical technique

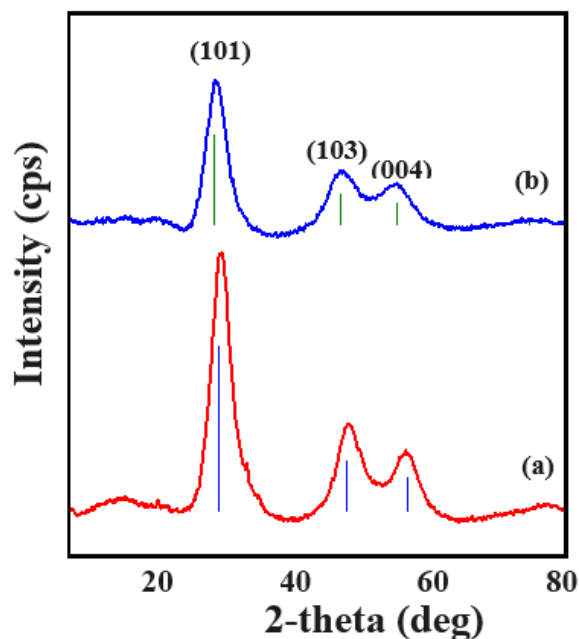


Fig. 1. XRD pattern of a)  $\text{Cd}_{0.2}\text{Zn}_{0.8}\text{S}/\text{PVA}$  and b)  $\text{Cd}_{0.4}\text{Zn}_{0.6}\text{S}/\text{PVA}$  by sonochemical technique.

XRD analysis of  $\text{Cd}_{0.2}\text{Zn}_{0.8}\text{S}/\text{PVA}$  and  $\text{Cd}_{0.4}\text{Zn}_{0.6}\text{S}/\text{PVA}$  based nanocomposite materials as nanoparticles shows peaks at  $2\theta=22.79^\circ$ ,  $46.81^\circ$ , and  $55.76^\circ$ , and  $2\theta=27.40^\circ$ ,  $45.82^\circ$ , and  $54.12^\circ$ , respectively. These peaks correspond to hexagonal phase of  $\text{Cd}_x\text{Zn}_{1-x}\text{S}$ , as evidenced by the Miller indices (101), (103), and (004), respectively (card number ICDD 00-049-1302) [1].

The diffraction pattern of nanocomposite materials, achieved by employing distinct capping agents to stabilize  $\text{Cd}_{0.4}\text{Zn}_{0.6}\text{S}$  based nanocomposite materials via sonochemical technique, is illustrated in Figure 2.

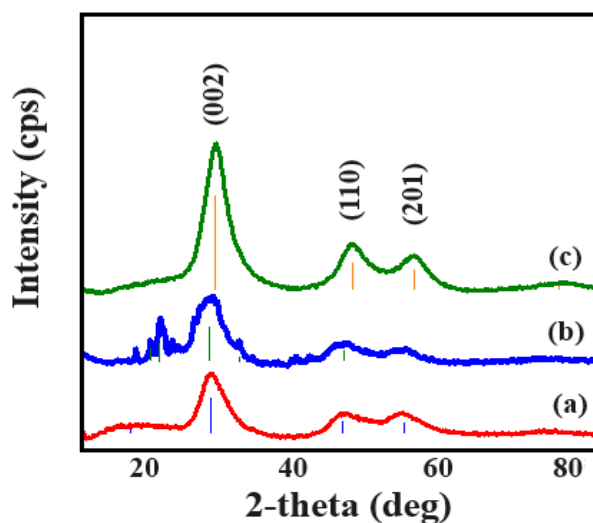


Fig. 2. XRD pattern of  $\text{Cd}_{0.4}\text{Zn}_{0.6}\text{S}$ -based nanocomposite materials as nanoparticles incorporating three stabilizers: a) PVA; b) 3-MPA; c) Styrene using the sonochemical technique.

Primary peaks identified in this context are located at  $2\theta=26.48^\circ$ ,  $44.78^\circ$ , and  $52.47^\circ$  for one set of nanocomposites,  $2\theta=27.66^\circ$ ,  $46.09^\circ$ , and  $54.44^\circ$  for another set, and  $2\theta=27.36^\circ$ ,  $44.72^\circ$ , and  $53.13^\circ$  for a third set synthesized using different stabilizers. These peaks align with the (101), (103), and (201) Miller indices, characteristic of the hexagonal phase of  $\text{Cd}_x\text{Zn}_{1-x}\text{S}$ . In comparison with literature data, these nanocomposites were found to correspond to ICDD card number 00-049-1302. The particle sizes for  $\text{Cd}_{0.4}\text{Zn}_{0.6}\text{S}$  which stabilized by PVA, 3-MPA and styrene is 7 nm, 5 nm and 9 nm, respectively. Thus, using different stabilizers under the same synthesis conditions resulted in a consistent structure, but the particle sizes varied. These differences were attributed to alterations in free Gibbs energy values due to interactions with the particles, depending on the stabilizer type. Essentially, the stabilizers, aimed at impeding the agglomeration of nanoparticles, exhibited distinct interactions based on their physical parameters, leading to varied nanoparticle sizes. Simultaneously, the surface tension force caused shifts in the energetic state of nanoparticles and stabilizers, contributing to alterations in the dimensions of the formed nanoparticles.

Figure 3 depicts the patterns obtained from XRD of  $\text{Cd}_x\text{Zn}_{1-x}\text{S}/\text{PVA}$ -based nanocomposite materials ( $x=0.1$  and  $0.2$ ) as thin films.

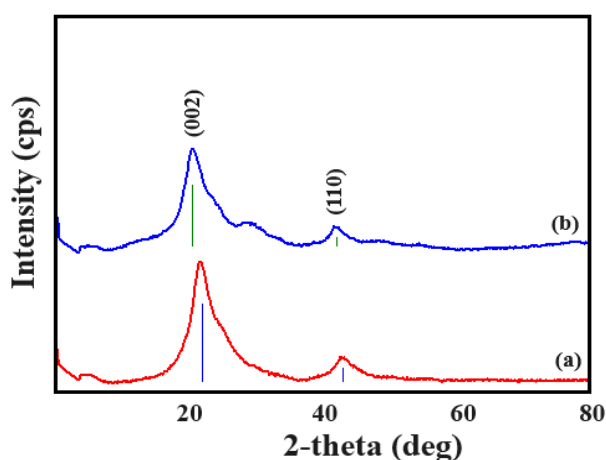


Fig. 3. XRD pattern for a)  $\text{Cd}_{0.1}\text{Zn}_{0.9}\text{S}/\text{PVA}$ ; b)  $\text{Cd}_{0.2}\text{Zn}_{0.8}\text{S}/\text{PVA}$  by SILAR technique.

Figure 3's peaks at  $2\theta \leq 22^\circ$  indicate the PVA matrix [2,3]. Peaks at  $2\theta = 26^\circ$  and  $43^\circ$  confirmed the presence of  $\text{Cd}_x\text{Zn}_{1-x}\text{S}$  solid complex (ICDD card number 00-049-1302). Furthermore, the structural investigation revealed that the compound had hexagonal symmetry, crystallizing on surfaces to the (002) and (110) indices. The  $26^\circ$  and  $44^\circ$  peaks in Figure 3 (a,b) were analyzed following the aforementioned quality analysis sequence, confirming their alignment with the hexagonal structure of the  $\text{Cd}_x\text{Zn}_{1-x}\text{S}$  compound. Notably, when the quantity of  $\text{Cd}^{2+}$  ions in the solution increased the diffraction peaks shifted to lower angles. Existing literature reports indicate that diffraction angles tend to shift towards higher angles with increased density of  $\text{Zn}^{2+}$  ions. According to the scientific literature [5], diffraction angles move towards smaller angles when the quantity of  $\text{Zn}^{2+}$  rises while the concentration of  $\text{Cd}^{2+}$  declines.

Generally, in the  $\text{Cd}_x\text{Zn}_{1-x}\text{S}$  structure, lattice constants increase with increasing value of  $x$  ( $a_0 = 0.386$ ,  $c_0 = 0.630$  when  $x = 0.16$ ;  $a_0 = 0.388$ ,  $c_0 = 0.632$  when  $x = 0.24$ ,  $a_0 = 0.32$  when  $x = 0.32$  0.390,  $c_0 = 0.634$ ;  $a_0 = 0.400$ ,  $c_0 = 0.653$  when  $x = 0.49$ ,  $a_0 = 0.403$ ,  $c_0 = 0.657$  when  $x = 0.84$ ,  $a_0 = 0.406$ ,  $c_0 = 0.660$  when  $x = 0.65$ ) [6,7]. The lattice constants of CdS in both the cubic (5.8320 Å) and hexagonal ( $a_0 = 4.160$  Å,  $c_0 = 6.756$  Å) phases are smaller than the lattice constants of ZnS (cubic – 5.420 Å, hexagonal –  $a_0 = 3.82$  Å,  $c_0 = 6.26$  Å) is large.

Both the sonochemical and SILAR technique produced  $\text{Cd}_x\text{Zn}_{1-x}\text{S}$ -based nanocomposite materials that, when obtained under normal conditions, formed in the hexagonal phase. This suggests that for the composite materials shown, less energy is required to formation the hexagonal phase. Thus, using a variety of synthesis techniques, this  $\text{Cd}_x\text{Zn}_{1-x}\text{S}$  solid solution is created in the hexagonal phase at room temperature and normal atmospheric pressure.

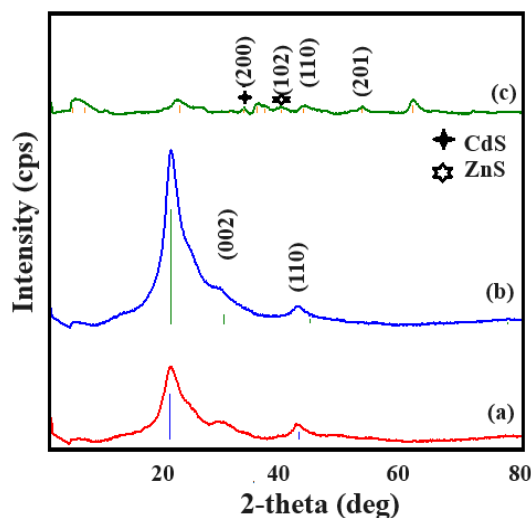


Fig. 4. XRD pattern of  $\text{Cd}_{0.2}\text{Zn}_{0.8}\text{S}$  which synthesized different temperature a)  $T = 25^\circ\text{C}$ ; b)  $T = 45^\circ\text{C}$ ; c)  $T = 65^\circ\text{C}$  by SILAR technique.

Figure 4 presents the XRD patterns of  $\text{Cd}_{0.2}\text{Zn}_{0.8}\text{S}/\text{PVA}$  nanocomposite samples obtained at various synthesis temperatures. Notably, the intensity of diffraction peaks observed at room temperature is lower compared to samples obtained at elevated temperatures. The structural analysis attributes the structure of samples synthesized at  $40^\circ\text{C}$  and  $65^\circ\text{C}$  to the hexagonal phase of the  $\text{Cd}_x\text{Zn}_{1-x}\text{S}$  compound, with diffraction angles of  $2\theta = 42.14^\circ$  and  $51.76^\circ$  corresponding to (110) and (201) Miller indices, respectively. Additionally, a newly observed peak at  $2\theta = 33.2^\circ$  in the diffraction pattern of  $\text{Cd}_{0.2}\text{Zn}_{0.8}\text{S}/\text{PVA}$  nanocomposites obtained at  $65^\circ\text{C}$  is related to the formation of CdS in the hexagonal phase, aligning with the (200) Miller index and corresponding to ICDD card number 80-0006 [8]. Another observed peak at  $2\theta = 38.4^\circ$ , indicative of a cubic structure, is attributed to the ZnS compound with the Miller index (102), corresponding to ICDD card number 65-1691 [9].

The diffraction spectrum shows the production of ternary CdZnS and binary CdS and ZnS compounds [10]. During the synthesis of  $\text{Cd}_{0.2}\text{Zn}_{0.8}\text{S}/\text{PVA}$  nanocomposites at  $65^\circ\text{C}$ , the production

of these materials (CdS, ZnS,  $Cd_xZ_{1-x}S$ ) was further confirmed by the band gap value. Analysis of the spectra revealed the more intense peaks of ternary CdZnS nanocomposites at 45°C. The crystalline's size decreased by the increasing of synthesis temperature (65°C). Variation of the observed diffraction pattern at different temperatures, while maintaining constant density, were attributed to the particle nucleation process, increased density of sorption centers, and activated joining processes within the polymer matrix under specific temperature conditions. Subsequent temperature elevation weakened the aggregation process, resulting in a reduction in particle size. This phenomenon related to effect of growth process's mobility due to the acceleration of chaotic movement of ions influence of the higher temperature, hindering the creation of a stable environment for their combination. Consequently, it was determined that particle sizes decrease up to a certain limit with the temperature increase ( $T=65^\circ\text{C}$ ).

A solid solution is characterized by the lattice constant. That is, CdZnS is determined by a constant lattice parameter despite the change in concentration. As the temperature increases, the dipole motion increases. At higher temperatures, the dipole's motion does not allow it to be ordered (irregularity in the sequence of anion and cation). The growth of chaotic motion prevents orderly arrangement and separate phases are formed.

PVA was annealed at a high temperature of 65°C, which produced the hexagonal phase of the CdZnS solid solution, the hexagonal phase of the CdS compound, and the cubic phase of the ZnS compound. This indicates that a mixed phase and a CdZnS solid solution were created here. Additionally, free  $Cd^{2+}$ ,  $Zn^{2+}$ , and  $S^{2-}$  ions present in the PVA sorption centers developed independently into binary CdS and ZnS due to temperature effect. In other words, unique reaction conditions—that is, a sufficiently high energy—are needed for the development of the cubic phase.

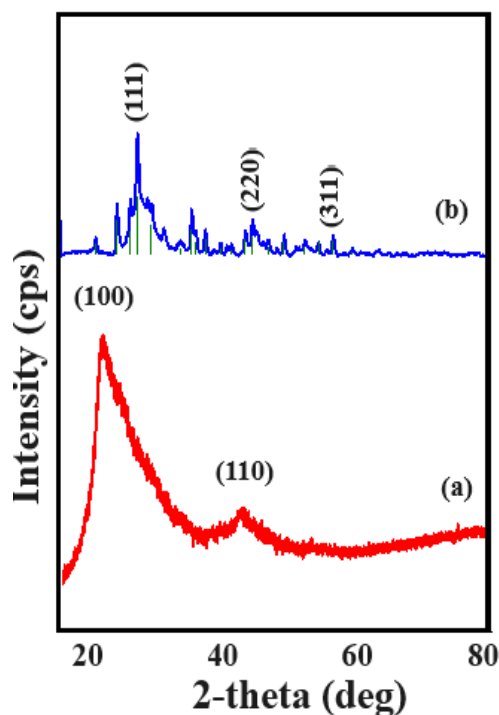


Fig. 5. XRD pattern of CdS by a) sonochemical technique; b) SILAR technique.

XRD patterns of CdS nanocomposites materials as nanoparticles by sonochemical technique (Fig.5.a) and as a thin film by SILAR technique (Fig.5.b) are illustrated in Figure 5. In Figure 5.a., the prominent observed peaks of CdS/PVA nanocomposite are 25.87°, 43.10°, and 53.07°. This structure is the peaks belonging to the CdS nanoparticles formed in the cubic phase, which corresponded to the JCPDS card number 10-0454 [11]. The observed peaks related to (111), (220), and (311) Miller indices, respectively [12].

It was observed that the XRD pattern of CdS/PVA thin film which synthesized via SILAR technique (Fig.5. b) corresponds to the JCPDS 41-1049 and the prominent peaks are  $2\theta=26^\circ$ ,  $37^\circ$ ,  $43^\circ$  peaks. These peaks indexed by the (100), (102), and (110) Miller indices and related to hexagonal phase.

When binary compounds were generated using the sonochemical approach, a cubic phase was formed in the production of CdS, while a hexagonal phase was formed when the SILAR technique was used. This suggests that the creation of the cubic phase requires a high temperature. On the other hand, most compounds generated at room temperature under typical conditions are hexagonal phase compounds.

For the crystal structure of the formed crystallite to change, the energy state in the center of formation needs to change. If the energy state changes, then the crystal structure will also change. Then, the particles may move from one crystal structure to another, for example, forming crystallites with a defect structure. This occurring mechanism depends on the interaction of the nanoparticle with the matrix as a result of the placement of the nanoparticle inside the matrix, as well as the effect of that temperature on the particles if they do not collapse at a certain temperature. Therefore, it isn't easy to think about the formation of this single-valued phase. Because it is somewhat difficult to calculate the total energy of the formed particle since it is a multifunctional variable.

### 3.2. Optical properties

$E_g$  value for all composite materials are calculated using the Tauc relation, which is based on the transmittance spectra obtained from the UV-Vis spectrometer study. Table 1 displays the  $E_g$  values for the samples.

Table 1.  $E_g$  value for nanocomposite materials (eV).

Materials	Sonochemical			SILAR		
	PVA	3-MPA	styrene	T=25°C	T=45°C	T=65°C
Cd <sub>0.1</sub> Zn <sub>0.9</sub> S	3.15	-	-	-	-	-
Cd <sub>0.2</sub> Zn <sub>0.8</sub> S	2.80	-	-	3.05	3.14	2.37
Cd <sub>0.4</sub> Zn <sub>0.6</sub> S	2.45	2.80	2.55	-	-	-
CdS	2.25	-	-	2.45	-	-

Table 1 shows that  $E_g$  for Cd<sub>x</sub>Zn<sub>1-x</sub>S/PVA (x=0.1, 0.2, 0.4, 1) based nanocomposite materials produced by the sonochemical technique was 3.15 eV, 2.80 eV, 2.45 eV, and 2.25 eV as x increased. In a Cd<sub>x</sub>Zn<sub>1-x</sub>S-based solid solution, the  $E_g$  value is reduced as Cd<sup>2+</sup> ions quantity rises. The results found that in some instances, the diameter of the nanoparticle's  $E_g$  is less than the bulk substance (2.42 eV) [13]. In the literature [14], changes of energy spectrum resulted in changes in the effective mass of charge carriers. Three stabilizers (PVA, 3-MPA, and styrene) were employed to analyse the influence of stabilizers on optical characteristics using a certain stoichiometric ratio.  $E_g$  value is 2.45 eV (Cd<sub>0.4</sub>Zn<sub>0.6</sub>S/PVA), 2.80 eV (Cd<sub>0.4</sub>Zn<sub>0.6</sub>S /3-MPA), and 2.55 eV (Cd<sub>0.4</sub>Zn<sub>0.6</sub>S /styrene). This change may be determined by the type of stabilizer used, whether it is polar or non-polar, its molecular weight and spatial structure, the influence of changing charge carriers' potential energy, and the effect of their effective mass.

In SILAR technique, during the synthesis process of Cd<sub>0.2</sub>Zn<sub>0.8</sub>S/PVA nanocomposite materials obtained at various grow temperature (45°C), the band gap values of nanoparticles slightly increased with increasing temperature (from 3.05 eV to 3.14 eV). Rising of grown temperature to 65°C led to a decrease in the  $E_g$  value (from 3.14 eV to 2.37 eV). It is evidence of defect structure of nanocomposite materials in the structure of nanoparticles, connection with the environment, and dimensions effect  $E_g$  value [14]. Differences were also found in the  $E_g$  values of CdS produced using two different procedures. The sonochemical approach yields CdS nanoparticles with a band gap of 2.25 eV, whereas the SILAR technique yields CdS thin films with an  $E_g$  value of 2.45. This variation in  $E_g$  value is due to a difference in crystallographic structure (cubic phase by sonochemical technique, hexagonal phase by SILAR technique). Thus, structures with a high degree of

crystallinity are generated by the sonochemical technique, while structures with a relatively low degree of crystallinity are formed by the SILAR technique.

In general,  $E_g$  value depends on many parameters. One of them is size dependence due to quantum size effects. At the same time, geometric dimensions of the nanocomposite materials and the outside surrounding can be affected to  $E_g$  value [15]. By the SILAR approach, CdS nanoparticles of 5.42 nm, while the sonochemical process yields CdS nanoparticles of 3.06 nm.

During the formation of particles, the interphase interaction also affects the physical properties of the particles. Crystal structure, interphase interactions, and particle sizes are parameters that affect physical properties. Depending on the type of stabilizer used, the formation of an additional layer (double electrical layer) can lead to a change in properties. In general, band gap value and other physical properties of particles depend not only on their size, but also on the environment surrounding it, the characteristics of the environment, the dipole moment, and the interaction mechanism of the charge carriers in the particle with the environment. So, these changes in the  $E_g$  value of the particles can vary depending on the width of the double electrical layer formed at the boundary between the two environments, depending on the nanocomposite material. At the same time, as a result of the interaction of the particle with the environment, defective structures can be formed and thus affect the potential energy of charge carriers. This can affect its  $E_g$  value and other physical properties.

### 3.3. FTIR spectrum

Figure 6 illustrates the IR spectrum of nanoparticles derived from  $Cd_xZn_{1-x}S$ -based nanocomposite materials using three different stabilizers through the sonochemical technique.

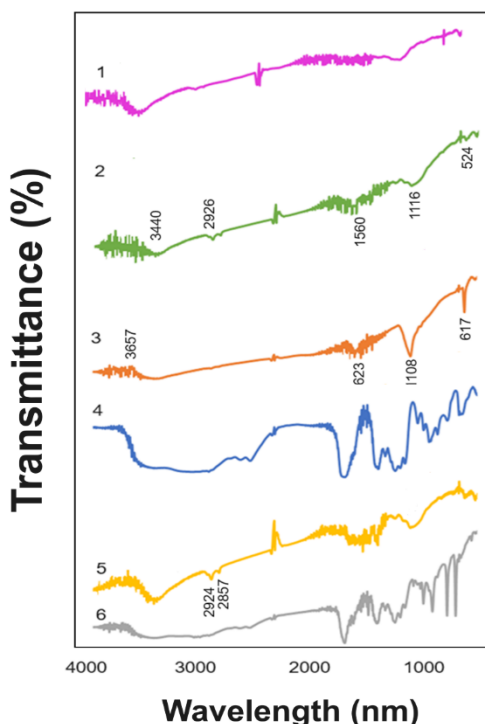


Fig. 6. IR spectrum of  $Cd_{0.4}Zn_{0.6}S$  based composite materials 1- $Cd_{0.4}Zn_{0.6}S/PVA$ ; 2-PVA; 3-  $Cd_{0.4}Zn_{0.6}S/3$ -MPA; 4-3-MPA; 5- $Cd_{0.4}Zn_{0.6}S/styrene$ ; 6-styrene.

In Figure 6, demonstrated IR spectra of  $Cd_{0.4}Zn_{0.6}S/PVA$  (Fig.6.1) and pure PVA (Fig.6.2). From the IR spectra of the  $Cd_{0.4}Zn_{0.6}S/PVA$  (Fig. 6.1), the peak at  $3440\text{ cm}^{-1}$  within the wide emission is ascribed to  $-OH$  groups, while the low-frequency emission at  $2926\text{ cm}^{-1}$  is related to the  $-CH_2-$  bond. The peak associated with the  $C-O$  is seen at  $1560\text{ cm}^{-1}$  and  $1116\text{ cm}^{-1}$ ,  $524\text{ cm}^{-1}$  is related to the  $C-H$  bond.

The FTIR spectra of the  $\text{Cd}_{0.4}\text{Zn}_{0.6}\text{S}/3\text{-MPA}$  nanocomposite is depicted in Figure 6.3. The O–H link peak is seen at a wavenumber of  $3657\text{ cm}^{-1}$ .  $1108\text{ cm}^{-1}$  is related to the C–O link, and C=O and S–C link are seen at  $1623\text{ cm}^{-1}$  and  $617\text{ cm}^{-1}$ , respectively [16]. Emission spectra of pristine MPA (Fig. 6.3 and Fig. 6.4), emissions at  $2659\text{ cm}^{-1}$  and  $2571\text{ cm}^{-1}$  are considered applicable to the S–H bond. The missing of certain bands in the IR spectra of the  $\text{Cd}_{0.4}\text{Zn}_{0.6}\text{S}/3\text{-MPA}$  nanocomposite is interpreted as being caused by the interaction of 3-MPA with the metallic component through the thiol group.

The IR spectra of the  $\text{Cd}_{0.4}\text{Zn}_{0.6}\text{S}/\text{styrene}$  is presented in Figure 6.5. The aromatic C–H link is observed at a wavenumber of  $2924\text{ cm}^{-1}$ . The low-intensity band at  $2857\text{ cm}^{-1}$  is considered related to the CH–CH<sub>2</sub> bond [17]. The peaks observed in  $\text{Cd}_{0.4}\text{Zn}_{0.6}\text{S}$  based nanocomposite materials which obtained various stabilizers at  $617\text{ cm}^{-1}$ ,  $617\text{ cm}^{-1}$ , and  $615\text{ cm}^{-1}$  wavenumber is associated with Cd–S and Zn–S bonds.

The optical characteristics of nanoparticles based on  $\text{Cd}_x\text{Zn}_{1-x}\text{S}/\text{PVA}$ , synthesized through the SILAR technique investigated using IR spectroscopy. Figure 7 displays the IR spectrum of both the pristine PVA and nanocomposite materials through the SILAR technique at various grown temperatures.

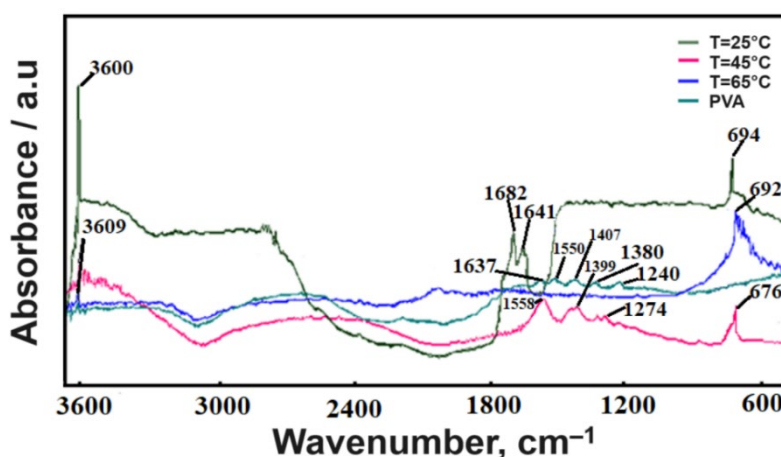


Fig. 7. FTIR spectra of  $\text{Cd}_{0.2}\text{Zn}_{0.8}\text{S}/\text{PVA}$ -based nanoparticles: pure PVA; synthesis at room temperature; synthesis at  $T=45^\circ\text{C}$ ; synthesis at  $T=65^\circ\text{C}$ .

The IR spectrum of the pristine PVA is depicted in Figure 7. The peaks seen in the range of  $3609\text{--}3600\text{ cm}^{-1}$  is attributed to –OH. The association is made connection with PVA and inclusion of water molecules in the composition. Peaks at  $1637\text{ cm}^{-1}$ ,  $1550\text{ cm}^{-1}$ ,  $1407\text{ cm}^{-1}$ ,  $1380\text{ cm}^{-1}$ , and  $1240\text{ cm}^{-1}$  seen in the pristine PVA related to the vibrations of C–O–H $\delta$  [18]. The distinct band at  $1682\text{ cm}^{-1}$  and  $1641\text{ cm}^{-1}$  ( $T=25^\circ\text{C}$ ) is attributed to the vibration of C=O. Peaks slightly moved to the higher wavenumber and diminished in intensity of the peaks ( $T=45^\circ\text{C}$ ). Such alterations are linked to the development of a ternary compound in the polymer, vibrational changes in the bonds, a decrease in energy, and therefore, decrease in the frequency of oscillatory motion. The peaks did not persist as the grown temperature was increased. This finding was confirmed by the evident degradation (softening) of the PVA at high temperatures. In pristine PVA spectra, peaks at  $694\text{ cm}^{-1}$ ,  $676\text{ cm}^{-1}$ , and  $692\text{ cm}^{-1}$  related to  $\text{Cd}_x\text{Zn}_{1-x}\text{S}$  evident in the spectrum of all nanocomposite materials. At  $T=65^\circ\text{C}$  grown temperature, multiple bands were seen in the background of the  $692\text{ cm}^{-1}$  peak. The phenomenon was attributed to the development of CdS and ZnS alongside the hybrid structure of  $\text{Cd}_x\text{Zn}_{1-x}\text{S}$  nanoparticles at these elevated temperatures.

### 3.4. Morphological analysis

Depending on the obtained technique, SEM is recognized as a highly significant technique for the comparative analysis of sample morphology. In this context, SEM images of nanocomposite materials prepared with various compositions using two techniques are presented in Figure 8.

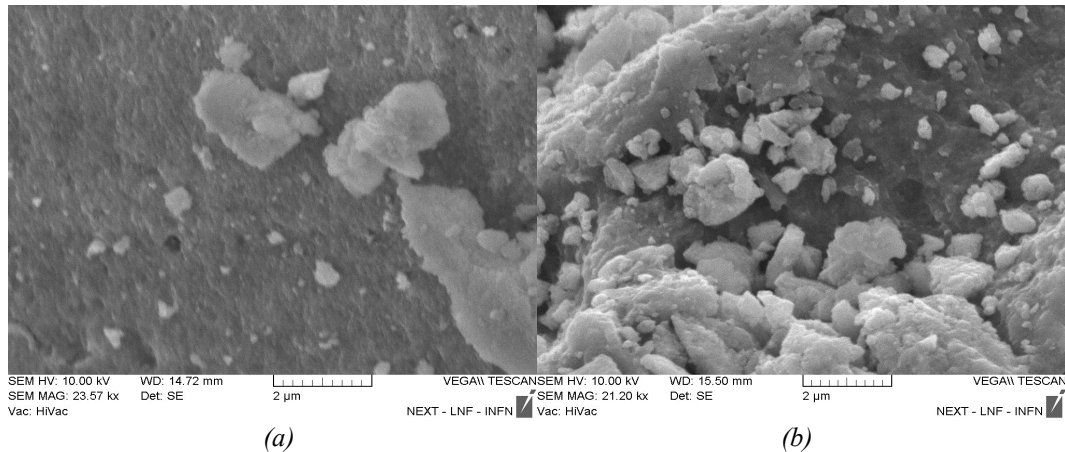


Fig. 8. SEM images of a)  $Cd_{0.2}Zn_{0.8}S/PVA$  and b)  $Cd_{0.4}Zn_{0.6}S/PVA$  nanocomposite samples obtained by sonochemical technique.

It can be seen from Figure 8, that the size of  $Cd_xZn_{1-x}S$  nanocomposite materials as nanoparticles synthesized by the sonochemical technique increased with the rises of  $Cd^{2+}$  quantity in the structure. In Figure 8. b, it is clear that large crystallites are formed. Thus, the ionic radius of  $Cd^{2+}$ ,  $Zn^{2+}$  is 0.95 Å and 0.79 Å, respectively [19]. So, the ionic radius of  $Cd^{2+}$  is larger than  $Zn^{2+}$ . In this regard, the formation of larger particles with a rise of  $Cd^{2+}$  quantity in the structure is related to the ionic radius of the particles.

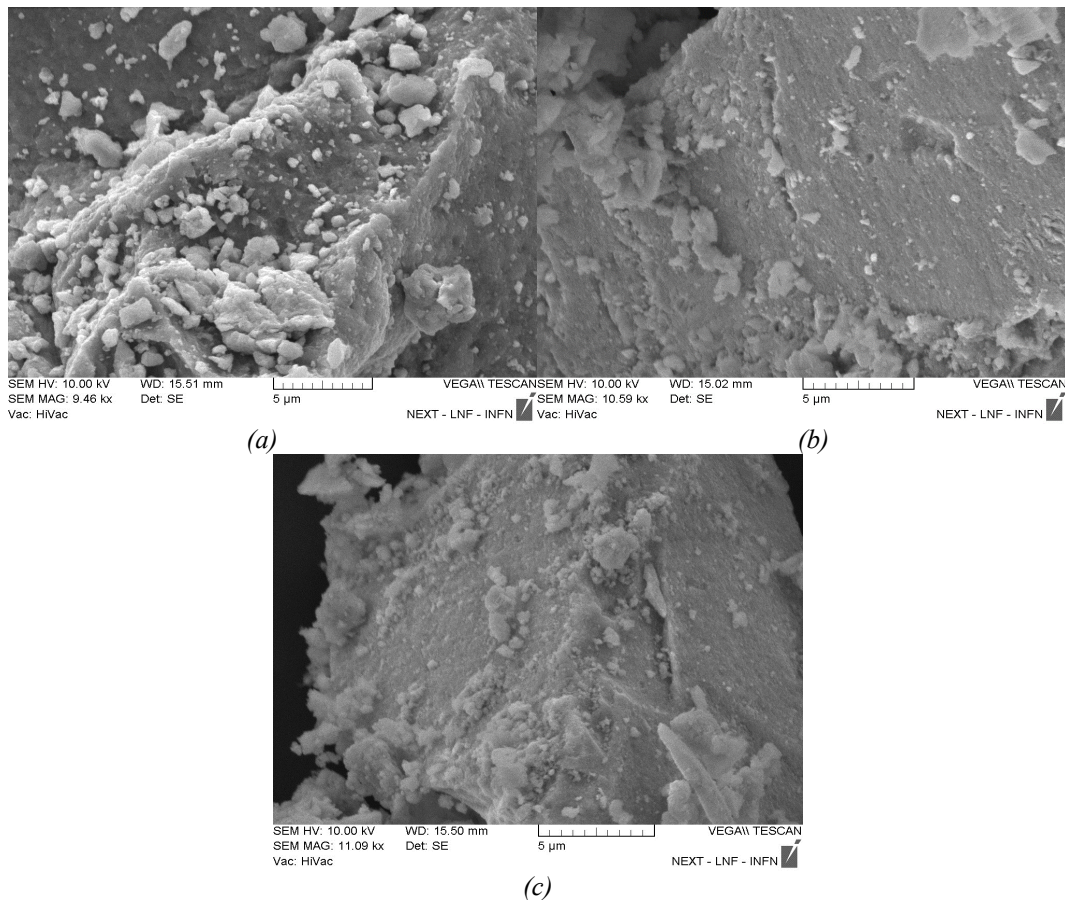


Fig. 9. SEM images of  $Cd_{0.4}Zn_{0.6}S$  by various stabilizers: a) PVA; b) 3-MPA; c) Styrene by sonochemical technique

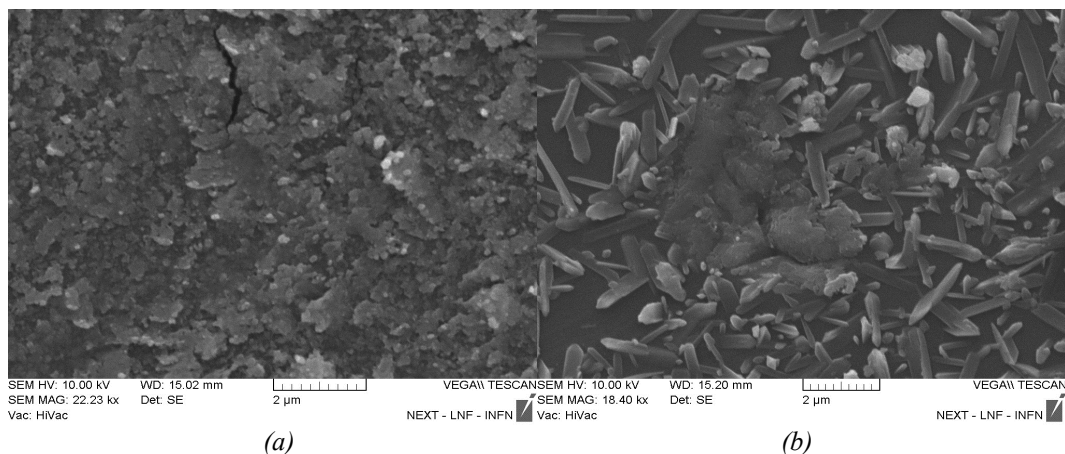


Fig. 10. SEM images of a)  $Cd_{0.1}Zn_{0.9}S$  and b)  $Cd_{0.2}Zn_{0.8}S$  by SILAR technique.

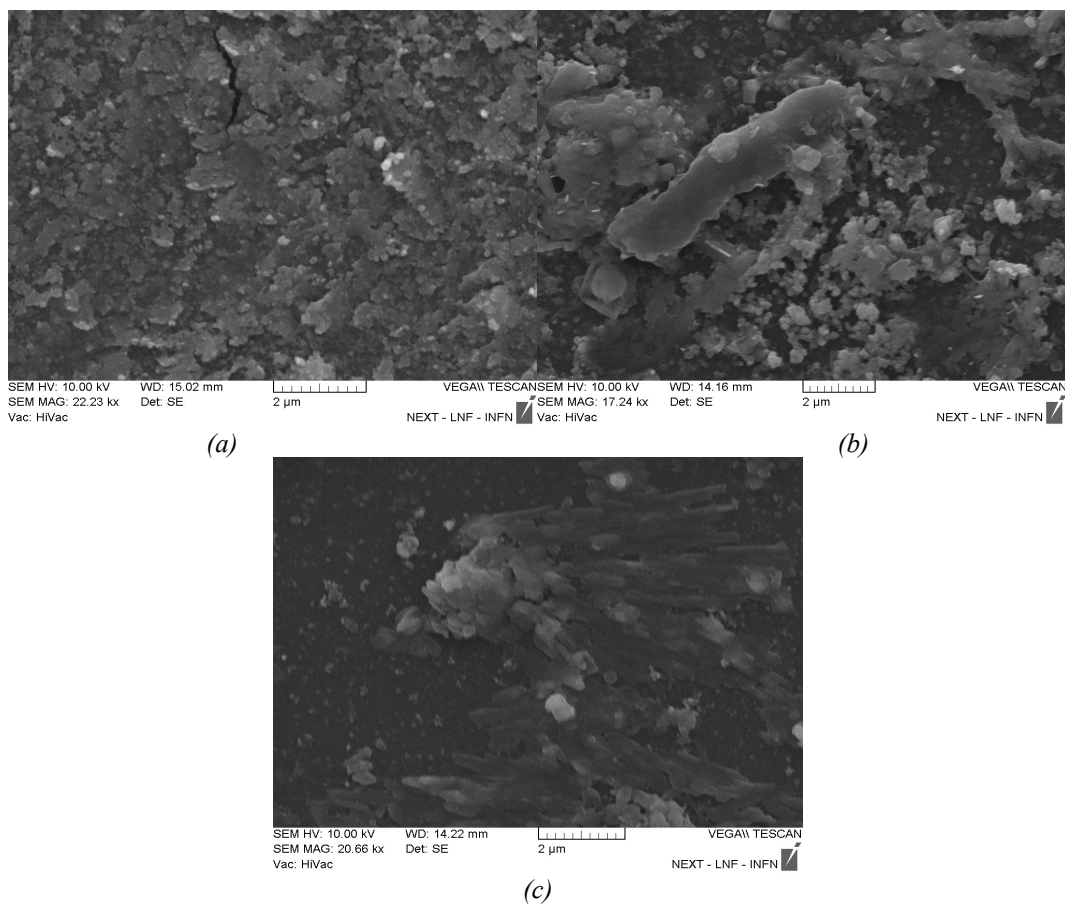


Fig. 11. SEM images of  $Cd_{0.2}Zn_{0.8}S$  which synthesized various temperature a)  $T=25^{\circ}C$ ; b)  $T=45^{\circ}C$ ; c)  $T=65^{\circ}C$  by SILAR technique.

Figure 9 shows SEM images of  $Cd_{0.4}Zn_{0.6}S$  nanocomposite materials which stabilized with various stabilizers. Here, in Figure 9.a,  $Cd_{0.4}Zn_{0.6}S$  /PVA nanocomposite materials are relatively larger,  $Cd_{0.4}Zn_{0.6}S$  /styrene (Fig. 9.c) is smaller than  $Cd_{0.4}Zn_{0.6}S$  /3-MPA (Fig. 9.b). We can observe the formation of smaller particles compared to other capping agents.

Figure 10 presents morphological analysis of  $Cd_{0.1}Zn_{0.9}S$ /PVA (Fig. 10. a) and  $Cd_{0.2}Zn_{0.8}S$ /PVA (Fig.10. b) nanocomposites by the SILAR technique. As mentioned, since the SILAR technique is based on the formation of crystallites in layers, it is obvious that these structures

are formed on the surface of PVA at small concentrations of  $\text{Cd}^{2+}$  ions. It is observed that these layered structures are separated from the outside of the PVA and was formed free-layered crystallites form.

Figure 11 shows morphological analysis of  $\text{Cd}_{0.2}\text{Zn}_{0.8}\text{S}/\text{PVA}$  nanocomposite materials which synthesized via SILAR technique at various grown temperatures.  $\text{Cd}_{0.2}\text{Zn}_{0.8}\text{S}/\text{PVA}$  obtained at  $T = 25^\circ\text{C}$  (Fig. 11.a) consists of nanoparticles attached to the PVA matrix surface.  $\text{Cd}_{0.2}\text{Zn}_{0.8}\text{S}/\text{PVA}$  nanocomposites synthesized at  $T=45^\circ\text{C}$  show that these crystallites are attached to the surface, and during the synthesis process at higher temperatures ( $T=65^\circ\text{C}$ ). These nanoparticles are completely attached to the surface of the PVA matrix (Fig. 11.b). This leads to the softening of PVA due to the melting temperature, and as a result, the nanoparticles also undergo various modifications on their surface.

In Figure 12 demonstrated CdS nanostructures obtaining by sonochemical (Fig.12.a) and SILAR technique (Fig.12.b).

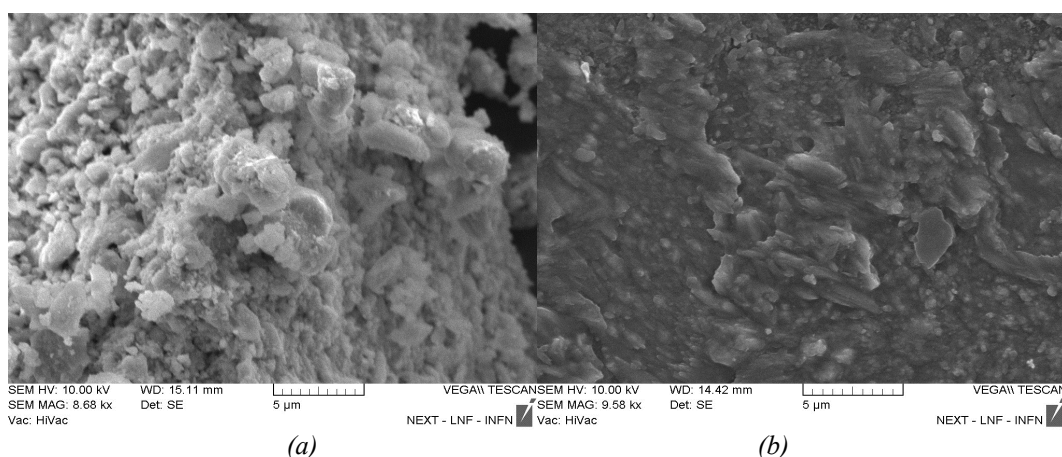


Fig. 12. SEM images of CdS by a) sonochemical technique; b) SILAR technique.

As mentioned above, since these two techniques are based on different physical properties, the size, distribution, and physical properties of nanoparticles, depending on the formation mechanism, are quite different from each other. Thus, with the sonochemical technique, it is possible to see that small-sized nanoparticles are formed freely, and with the SILAR technique, crystallites are formed in a layered form.

#### 4. Conclusion

$\text{Cd}_x\text{Zn}_{1-x}\text{S}$ -based nanocomposite materials were synthesized by SILAR technique at different synthesis temperatures (using PVA-polymer matrix as a substrate). At the same time,  $\text{Cd}_x\text{Zn}_{1-x}\text{S}$  based nanocomposite materials were synthesized using different stabilizers (PVA, 3-MPA and styrene). It was determined that in both synthesis techniques, ternary compounds are mainly formed hexagonal structure at  $T=25^\circ\text{C}$ .

During synthesis of binary compounds, compounds are formed in the hexagonal or cubic phase, depending on the technique used. At the same time, based on the results obtained from the XRD results, during the synthesis of ternary compounds at low temperatures, the hexagonal phase is formed, and at higher temperatures, binary compounds are formed in the cubic phase. From this, it can be concluded that the formation of the hexagonal phase in ternary compounds consumes less energy and is easily formed. During the comparison of the  $E_g$  values of the samples, it was determined that when the  $\text{Cd}_x\text{Zn}_{1-x}\text{S}$  compound was synthesized by different techniques (for the same  $x$  value), different values were obtained.

Thus, the  $E_g$  value for the  $Cd_{0.2}Zn_{0.8}S/PVA$  composite was 2.80 eV for the sonochemical technique, and 3.05 eV for the SILAR technique. At the same time, this also happened in binary combinations.  $E_g$  value for CdS yielded by sonochemical technique is 2.25 eV, and for SILAR technique is 2.45 eV. It was determined from the morphological analysis compounds obtained by sonochemical technique is spherical, while the nanocomposite materials obtained by the SILAR technique are layered. These are due to differences in the synthesis technique used.

## References

- [1] Gahramanli, L., Muradov, M., Kukovecz, Á., Balayeva, O., Eyvazova, G., *Inorganic and Nano-Metal Chemistry*, 50(9), 808-815 (2020); <http://dx.doi.org/10.1080/24701556.2020.1725050>
- [2] Krishnakumar, V., Shanmugam, G., Nagalakshmi, R., *Journal of Physics D: Applied Physics*, 45(16), 165102, (2012); <http://dx.doi.org/10.1088/0022-3727/45/16/165102>
- [3] Nasar, G., Khan, M. S., & Khalil, U., *J. Pak. Mater. Soc.*, 3(2), 67 (2009)
- [4] Mohammed, K. A., Al Hasan, N. H. J., Al-Ameer, L. R., Abdul-Zahra, D. S., Dwivedi, Y. D., Salem, K. H., Alkhafaji, M. A, *Chalcogenide Letters*, 20(8) (2023); <https://doi.org/10.15251/CL.2023.208.599>
- [5] Thahab, S. M., Alkhayat, A. H. O., Saleh, S. M., *Optik*, 125(18), 5112-5115, (2014); <https://doi.org/10.1016/j.ijleo.2014.05.014>
- [6] Ballentyne D.W.G. Ray R.-*Physica* –1961.27, –337 p.; [https://doi.org/10.1016/0031-8914\(61\)90106-9](https://doi.org/10.1016/0031-8914(61)90106-9)
- [7] Congiu A. *Nuovo Cimento*, A. Congiu, P. Manca, A. Spiga, –1971. B5, –204 p.; <https://doi.org/10.1007/BF02738148>
- [8] Laera, A. M., Resta, V., Piscopiello, E., Miceli, V., Schioppa, M., Scalone, A. G., Tapfer, L, *Nanoscale research letters*, 8(1), 382 (2013); <https://doi.org/10.1186/1556-276X-8-382>
- [9] Soltani, N., Saion, E., Hussein, M. Z., Erfani, M., Abedini, A., Bahmanrokh, G., Vaziri, P, *International journal of molecular sciences*, 13(10), 12242-12258 (2012); <https://doi.org/10.3390/ijms131012242>
- [10] Gahramanli, L. R., Muradov, M. B., Balayeva, O. O., Eyvazova, G. M., Mirsultanova, R. M., *Materials Research Bulletin*, 137, 111162 (2021); <https://doi.org/10.1016/j.materresbull.2020.111162>
- [11] Gahramanli, L., Muradov, M., Kukovecz, A., Balayeva, O., Eyvazova, G., & Nuriyeva, S., *Journal of Non-Oxide Glasses Vol*, 11(4), 57-63 (2019)
- [12] Gahramanli, L., Muradov, M., Kukovecz, Á., Balayeva, O., Eyvazova, G., Huseynli, S., Shirinova, H., *Dimensional Systems*, 3, 19 (2019)
- [13] Biswas, A., Meher, S. R., & Kaushik, D. K. *Journal of Physics: Conference Series* (Vol. 2267, No. 1, p. 012155) (2022); <https://doi.org/10.1088/1742-6596/2267/1/012155>
- [14] Muradov, M. B., Eyvazova, G. M., Turan, R., & Maharramov, A. M., *Optoelectronics and Advanced Materials-Rapid Communications*, (2008);
- [15] Gahramanli, L., Muradov, M., Azizian, Y., Eyvazova, G., & Balayeva, O., *International Journal of Modern Physics B*, 37(11), 2350103 (2023); <https://doi.org/10.1142/S0217979223501035>
- [16] Muradov, M. B., Balayeva, O. O., Azizov, A. A., Maharramov, A. M., Qahramanli, L. R., Eyvazova, G. M., Aghamaliyev, Z. A, *Infrared Physics & Technology*, 89, 255-262 (2018); <https://doi.org/10.1016/j.infrared.2018.01.014>
- [17] Choi, J., Kim, K., Han, H. S., Hwang, M. P., & Lee, K. H. *Bulletin of the Korean Chemical Society*, 35(1), 35-38 (2014); <https://dx.doi.org/10.5012/bkcs.2014.35.1.35>
- [18] Тарасевич Б.Н. ИК спектры основных классов органических соединений. Справочные материалы, – Москва, – 2012, 55 с.
- [19] Ashith, V. K., Priya, K., AV, M. A., Keshav, R., Rao, G. K., Mahesha, M. G., *Materials Research Express*, 7(2), 026404 (2020); <https://dx.doi.org/10.1088/2053-1591/ab5ec4>